

# Toward a Damping-Robust Optimized Schwarz Waveform Relaxation Method for the Kelvin–Voigt Viscoelastic Wave Equation

Fu Li<sup>[0009–0005–1304–930X]</sup>,  
Yingxiang Xu<sup>[0000–0001–7994–5274]</sup>

## 1 Introduction

The Schwarz waveform relaxation algorithm has emerged as an efficient parallel-in-time method for solving evolution problems, demonstrating significant potential since its inception [10, 11, 12]. By decomposing the spatial domain into subdomains and solving time-dependent problems iteratively and independently on these subdomains, this algorithm facilitates parallelism in both space and time. The transmission conditions governing the exchange of information at the interfaces between subdomains are pivotal to the convergence performance of the algorithm. To accelerate the convergence of the classical Schwarz waveform relaxation (SWR) method, the optimized Schwarz waveform relaxation (OSWR) method was developed. It employs transmission conditions tailored to the physical properties of the underlying partial differential equations, which markedly accelerates the iterative process. This approach has been successfully applied to various models, including diffusion equations [2, 4, 9], wave equations [7, 8], and multi-physics coupling problems [3, 13].

In this paper, we investigate the OSWR method for the one-dimensional Kelvin–Voigt viscoelastic wave equation

$$\begin{aligned} \partial_{tt}u - \varepsilon \partial_{txx}u - \gamma \partial_{xx}u &= f, & \text{in } \Omega \times (0, T], \\ u(\cdot, 0) &= \psi_1, & \text{in } \Omega, \\ \partial_t u(\cdot, 0) &= \psi_2, & \text{in } \Omega, \\ u &= \phi, & \text{on } \partial\Omega \times (0, T], \end{aligned} \tag{1}$$

with particular focus on the algorithm’s robustness with respect to the damping coefficient  $\varepsilon$ , as the damping strength varies from  $10^{-4}$  for the Mantle P-waves [1]

---

Fu Li  
School of Mathematics and Statistics, Northeast Normal University, Changchun 130024, China,  
e-mail: lif097@nenu.edu.cn

Yingxiang Xu  
School of Mathematics and Statistics, Changchun University of Technology, Changchun 130012,  
China & School of Mathematics and Statistics, Northeast Normal University, Changchun 130024,  
China, e-mail: yxxu@nenu.edu.cn

to  $10^6$  for the glassy polymer [5]. Existing analysis [14] demonstrated that the wave transmission condition (c.f. Section 2) exhibits good performance exclusively in the weakly damped regime (small  $\varepsilon$ ), while the Robin transmission condition (c.f. Section 2) proves more effective under strongly damped conditions (large  $\varepsilon$ ). This observed dichotomy underscores the necessity for developing a unified computational framework that ensures robustness across the complete spectrum of  $\varepsilon$  values. To bridge this methodological gap, we herein propose and briefly analyze the OSWR algorithm incorporating a newly-designed two-sided characteristic transmission condition, specifically engineered to enhance algorithmic adaptability and convergence properties in typical application scenarios across the damping parameter domain.

### 2 Optimized Schwarz waveform relaxation algorithm

For ease of analysis, we assume that the spatial domain is an infinite domain  $\Omega = \mathbb{R}$ , which is decomposed as  $\overline{\Omega} = \overline{\Omega}_1 \cup \overline{\Omega}_2$  with  $\Omega_1 = (-\infty, L)$  and  $\Omega_2 = (0, +\infty)$ , where  $L \geq 0$  indicates the overlap between subdomains that should be small to save the computation. Define  $\Gamma_1 = \{L\}$  and  $\Gamma_2 = \{0\}$ . The OSWR algorithm for the model problem (1) reads: iteratively calculating for  $n = 1, 2, \dots$  until convergence

$$\begin{cases} \partial_{tt}u_j^n - \varepsilon\partial_{txx}u_j^n - \gamma\partial_{xx}u_j^n = f, & \text{in } \Omega_j \times (0, T], \\ (-1)^{3-j}\partial_x u_j^n + S_j u_j^n = g_j^n, & \text{on } \Gamma_j \times (0, T], \\ u_j^n(\cdot, 0) = \psi_1, & \text{in } \Omega_j, \\ \partial_t u_j^n(\cdot, 0) = \psi_2, & \text{in } \Omega_j, \end{cases} \tag{2}$$

where

$$g_j^n = (-1)^{3-j}\partial_x u_{3-j}^{n-1} + S_j u_{3-j}^{n-1}, \text{ on } \Gamma_j \times (0, T],$$

and  $S_j, j = 1, 2$  are linear operators in time. By linearity, it suffices to consider only the case  $f = 0$ , which corresponds to analyzing the error equation directly. Taking a Fourier transform of the governing equations in (2) in the time direction gives

$$\begin{cases} -k^2\hat{u}_j^n - ik\varepsilon\partial_{xx}\hat{u}_j^n - \gamma\partial_{xx}\hat{u}_j^n = 0, & \text{in } \Omega_j \times \mathbb{K}, \\ (-1)^{3-j}\partial_x\hat{u}_j^n + \sigma_j\hat{u}_j^n = (-1)^{3-j}\partial_x\hat{u}_{3-j}^{n-1} + \sigma_j\hat{u}_{3-j}^{n-1}, & \text{on } \Gamma_j \times \mathbb{K}, \end{cases} \tag{3}$$

where  $\sigma_j(k)$  are Fourier symbols of the operators  $S_j$ ,  $k$  represents the Fourier frequency, and  $\mathbb{K}$  is the set of all admissible frequencies involved in a practical calculation. Solving (3), a short computation (see [14]) gives the convergence factor

$$\rho(k, L, \sigma_1, \sigma_2) = \left| \frac{-\lambda + \sigma_1}{\lambda + \sigma_1} \cdot \frac{-\lambda + \sigma_2}{\lambda + \sigma_2} \right| \cdot |e^{-2\lambda L}|,$$

where  $\lambda(k) = \sqrt{\frac{-k^2}{ik\varepsilon + \gamma}} = \frac{|k|\sqrt{\sqrt{\gamma^2 + \varepsilon^2 k^2} - \gamma}}{\sqrt{2}\sqrt{\gamma^2 + \varepsilon^2 k^2}} + i \frac{k\sqrt{\sqrt{\gamma^2 + \varepsilon^2 k^2} + \gamma}}{\sqrt{2}\sqrt{\gamma^2 + \varepsilon^2 k^2}} =: a(k) + ib(k).$

We would like to approximate the optimal Fourier symbols  $\sigma_j^* := \lambda(k)$  using linear functions of  $ik$ , i.e.,  $\sigma_j = p_j + q_j ik$ , which correspond to the following interface operators  $S_j = p_j + q_j \partial_t$  and can avoid complex number calculations. The convergence factor of the OSWR algorithm (2) now reads

$$\rho(k, L, p_1, p_2, q_1, q_2) = \sqrt{\frac{(a - p_1)^2 + (b - q_1 k)^2}{(a + p_1)^2 + (b + q_1 k)^2} \cdot \frac{(a - p_2)^2 + (b - q_2 k)^2}{(a + p_2)^2 + (b + q_2 k)^2}} e^{-2aL}.$$

The following three transmission conditions are included in this setting [14]: the Robin condition  $p_j = p, q_j = 0$  approximates only the real part  $a(k)$ , the characteristic condition  $p_j = 0, q_j = q$  (specifically,  $q = \frac{1}{\sqrt{\gamma}}$  defines the optimal condition for wave equation [8]), and will be referred as the wave condition hereafter) approximates only the imaginary part  $b(k)$  and the mixed condition  $p_j = p, q_j = q$  simultaneously approximates both. The left panel of Fig. 1 reveals that a homogeneous linear function of  $k$  approximates the imaginary part  $b(k)$  significantly better than a constant function approximates the real part  $a(k)$ , even when  $a(k)$  is substantially smaller. Note that large  $\varepsilon$  diminishes the difference between  $a(k)$  and  $b(k)$ , will even enhance this observation. Moreover, the right panel shows that for small  $\varepsilon$ ,  $b(k)$  is significantly larger than  $a(k)$ , highlighting the critical importance of approximating the imaginary part. Consequently, the characteristic condition is expected to considerably outperform the Robin condition, especially for small  $\varepsilon$ . Although the mixed condition approximates both the real and imaginary parts simultaneously, it is observed requiring impractically small mesh sizes to ensure good performance under weak damping scenarios, this is because the third maximum of its convergence factor reaches the asymptotic regime very late for  $\varepsilon$  small [14]. Based on the above analysis, while maintaining real-valued computations, the homogeneous linear approximation targeting the imaginary part  $b(k)$  demonstrates clear advantages. Therefore, to be more efficient, this paper studies the two-sided characteristic transmission condition with  $p_j = 0$  and  $q_1 \neq q_2$ , whose convergence factor is given by

$$\rho_{2C}(k, L, q_1, q_2) = \sqrt{\frac{a^2 + (b - q_1 k)^2}{a^2 + (b + q_1 k)^2} \cdot \frac{a^2 + (b - q_2 k)^2}{a^2 + (b + q_2 k)^2}} e^{-2aL}.$$

The OSWR methods then choose the free parameters  $q_j \geq 0, j = 1, 2$ , towards the best possible performance, by minimizing the convergence factor over all frequencies relevant to the problem

$$\min_{q_j \geq 0} \max_{k \in \mathbb{K}} \rho_{2C}(k, L, q_1, q_2), \quad (4)$$

where we comment that only positive Fourier frequencies should be considered, i.e.,  $\mathbb{K} = [k_{min}, k_{max}]$  with  $k_{min}$  typically estimated as  $k_{min} = \frac{\pi}{T}$  and  $k_{max}$  as  $k_{max} = \frac{\pi}{\tau}$ , where  $\tau$  is the time step size, since  $\rho_{2C}$  is symmetric in  $k$  due to the presence of the damping term  $-\varepsilon \partial_{t,x} u$ , which essentially differs from the classical wave equation where the convergence factor is asymmetric in  $k$ .

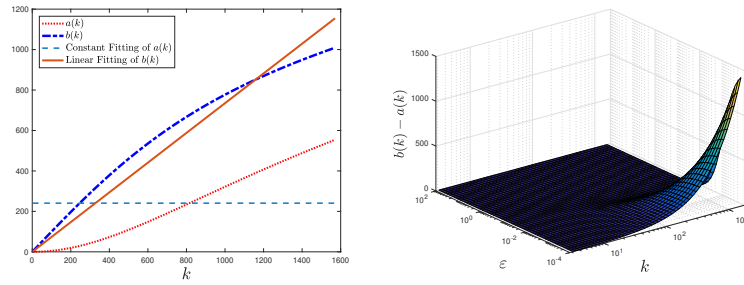


**Fig. 1** Left: for  $\varepsilon = 0.001, \gamma = 1$ , the  $a(k)$  and its least-squares fitting by a constant, and the  $b(k)$  and its least-squares fitting by a homogeneous linear function. Right: the difference between  $b(k)$  and  $a(k)$  as a function of  $\varepsilon$  and  $k$ .

### 3 Two-sided characteristic transmission conditions

In this section, we investigate the convergence performance of the OSWR algorithm with two-sided characteristic transmission conditions at the continuous level. In fact, the min-max problem (4) is equivalent to

$$\min_{q_1, q_2 > 0} \max_{k \in \mathbb{K}} \hat{\rho}_{2C}(k, L, q_1, q_2), \tag{5}$$

where  $\hat{\rho}_{2C} := \rho_{2C}^2$ . To help our analysis, we introduce the following approximate convergence factor for sufficiently large  $k > 0$

$$\tilde{\rho}_{2C}(k, L, q_1, q_2) = \frac{\tilde{b}^2 + (\tilde{b} - q_1 k)^2}{\tilde{b}^2 + (\tilde{b} + q_1 k)^2} \cdot \frac{\tilde{b}^2 + (\tilde{b} - q_2 k)^2}{\tilde{b}^2 + (\tilde{b} + q_2 k)^2} e^{-4\tilde{b}L}, \tag{6}$$

where  $\tilde{b} = \sqrt{\frac{k}{2\varepsilon}}$ . It can be derived that  $\tilde{\rho}_{2C} = \hat{\rho}_{2C} + O(\frac{L}{\sqrt{k}})$  holds for large  $k$  [14].

**Lemma 1** Assuming  $q_1 < q_2$ . As a function of  $k$ , the approximate convergence factor  $\tilde{\rho}_{2C}(k, L, q_1, q_2)$  defined in (6) has four critical points for  $k > 0$  at which it attains local extrema: two local minima at  $k = \underline{k}_1$  and  $k = \underline{k}_2$ , and two local maxima at  $k = \bar{k}_1$  and  $k = \bar{k}_2$ . Their asymptotic behaviors for small  $L$  are given by:

$$\underline{k}_1 \sim \frac{1}{\varepsilon q_2^2}, \bar{k}_1 \sim \frac{1}{\varepsilon q_1 q_2}, \underline{k}_3 \sim \frac{1}{\varepsilon q_1^2}, \bar{k}_4 \sim \frac{1}{q_1 L}.$$

*Proof.* The proof is similar to that of Theorem 4.12 in [2], and we omit it here.  $\square$

**Theorem 1 (Two-sided characteristic transmission conditions, overlapping case)**  
 Let  $L = C_1 h$  and  $\tau = C_2 h^\delta$  with  $h$  being the spatial mesh size and  $\tau$  the time step. The solution to the min-max problem (5) for sufficiently small  $h$  is given as follows

$$\begin{cases} q_1^* = 2\varepsilon^{-\frac{3}{5}} \varsigma_{\min}^{-\frac{2}{5}} C_1^{\frac{3}{5}} h^{\frac{3}{5}}, \\ q_2^* = 4\varepsilon^{-\frac{1}{5}} \varsigma_{\min}^{-\frac{1}{5}} C_1^{\frac{1}{5}} h^{\frac{1}{5}}, \end{cases} \quad \text{if } \delta > \frac{8}{5}, \text{ or } \delta = \frac{8}{5} \text{ and } C_1 \geq C_{2C},$$

$$\begin{cases} q_1^* = 2^{-2} \varsigma_{\min}^2 \tilde{C}_q^3 (C_1 h)^{\frac{3}{5}}, \\ q_2^* = 2\tilde{C}_q (C_1 h)^{\frac{1}{5}}, \end{cases} \quad \text{if } \delta = \frac{8}{5} \text{ and } C_1 < C_{2C},$$

$$\begin{cases} q_1^* = 2^{-\frac{1}{8}} (\varepsilon\pi)^{-\frac{3}{8}} C_2^{\frac{3}{8}} \varsigma_{\min}^{-\frac{1}{4}} h^{\frac{3\delta}{8}}, \\ q_2^* = 2 \cdot 2^{\frac{5}{8}} (\varepsilon\pi)^{-\frac{1}{8}} C_2^{\frac{1}{8}} \varsigma_{\min}^{-\frac{3}{4}} h^{\frac{\delta}{8}}, \end{cases} \quad \text{if } 0 < \delta < \frac{8}{5},$$

where  $\varsigma_{\min} = 4k_{\min}a_{\min}/(a_{\min}^2 + b_{\min}^2)$ , with  $a_{\min} = a(k_{\min})$ ,  $b_{\min} = b(k_{\min})$ ,  $C_{2C} = 2^{-\frac{5}{8}}\pi^{-\frac{5}{8}}C_2^{\frac{5}{8}}\varepsilon^{\frac{3}{8}}\varsigma_{\min}^{\frac{1}{4}}$ , and  $\tilde{C}_q$  is the unique positive root of the polynomial

$$P(\xi) = (\varepsilon\pi C_2)^{\frac{1}{2}} \varsigma_{\min}^3 C_1^{\frac{4}{5}} \xi^4 - \sqrt{2}\pi \varsigma_{\min}^2 C_1^{\frac{8}{5}} \xi^2 - 4\sqrt{2}C_2.$$

Moreover, for sufficiently small  $h$ , the corresponding convergence factor satisfies the following asymptotic estimates

$$\max_{k \in \mathbb{K}} \hat{\rho}_{2C}(k, L, q_1^*, q_2^*) = \begin{cases} 1 - 4\varepsilon^{-\frac{1}{5}} \varsigma_{\min}^{\frac{1}{5}} C_1^{\frac{1}{5}} h^{\frac{1}{5}} + O(h^{\frac{2}{5}}), & \text{if } \delta > \frac{8}{5}, \text{ or } \delta = \frac{8}{5} \text{ and } C_1 \geq C_{2C}, \\ 1 - 2\varsigma_{\min} \tilde{C}_q C_1^{\frac{1}{5}} h^{\frac{1}{5}} + O(h^{\frac{2}{5}}), & \text{if } \delta = \frac{8}{5} \text{ and } C_1 < C_{2C}, \\ 1 - 2 \cdot 2^{\frac{5}{8}} (\varepsilon\pi)^{-\frac{1}{8}} C_2^{\frac{1}{8}} \varsigma_{\min}^{\frac{1}{4}} h^{\frac{\delta}{8}} + O(h^{\frac{\delta}{4}}), & \text{if } 0 < \delta < \frac{8}{5}. \end{cases}$$

*Proof.* A sketch of the proof can be outlined in four steps:

**1. Determining  $q_1^* = C_{q_1} L^{\beta_1}$ ,  $q_2^* = C_{q_2} L^{\beta_2}$  via equi-oscillation:**

- The equi-oscillation problem is solved over  $\mathbb{K} = [k_{\min}, k_{\max}]$ , where the interior maximum points of the convergence factor  $\hat{\rho}_{2C}(k, L, q_1, q_2)$  are identified in Lemma 1, and are asymptotically given by

$$\bar{k}_1^* \sim \frac{1}{\varepsilon q_1^* q_2^*} = (\varepsilon C_{q_1} C_{q_2})^{-1} L^{-(\beta_1 + \beta_2)}, \quad \bar{k}_2^* \sim \frac{1}{q_1^* L} = C_{q_1}^{-1} L^{-(1 + \beta_1)}.$$

- Depending on the relative position of  $k_{\max} = \pi/(C_2 h^\delta)$  and  $\bar{k}_2^*$ , two regimes are identified:
  - $k_{\max} \geq \bar{k}_2^*$ . Equi-oscillate  $\hat{\rho}_{2C}$  between  $k_{\min}$ ,  $\bar{k}_1^*$  and  $\bar{k}_2^*$ .
  - $k_{\max} < \bar{k}_2^*$ . Equi-oscillate  $\hat{\rho}_{2C}$  between  $k_{\min}$ ,  $\bar{k}_1^*$  and  $k_{\max}$ .
- 2. **Finding the asymptotic locations of the local maxima:** it is shown that  $\hat{\rho}_{2C}(k, L, q_1, q_2)$  asymptotically attains its local maxima at  $k_{\min}$ ,  $\bar{k}_1^*$  and  $\bar{k}_2^*$ .
- 3. **Showing the optimality of  $q_1^*, q_2^*$  in an asymptotic sense:** any parameter pair  $(q_1, q_2) = (C_{q_1} L^{\beta_1}, C_{q_2} L^{\beta_2})$  other than  $(q_1^*, q_2^*)$  is shown to produce a larger maximum value of  $\hat{\rho}_{2C}$ . All we need is to show that if  $(q_1, q_2) \neq (q_1^*, q_2^*)$ , then there exists a  $k^*$  such that for  $h > 0$  small enough

$$\hat{\rho}_{2C}(k^*, L, q_1, q_2) > \max_k \hat{\rho}_{2C}(k, L, q_1^*, q_2^*) = \hat{\rho}_{2C}(k_{min}, L, q_1^*, q_2^*).$$

4. **Asymptotic expansion:** expanding the convergence factor  $\hat{\rho}_{2C}(k_{min}, L, q_1^*, q_2^*)$  in  $h$  to obtain the asymptotic convergence rate estimate.  $\square$

A similar analysis for the non-overlapping case yields the following result.

**Theorem 2 (Two-sided characteristic transmission conditions, non-overlapping case)** *For the non-overlapping case  $L = 0$ , if  $k_{max}$  is large enough, the parameters*

$$\begin{cases} q_1^* = 2 \cdot 2^{\frac{5}{8}} \varepsilon^{-\frac{1}{8}} S_{min}^{-\frac{3}{4}} k_{max}^{-\frac{1}{8}} \\ q_2^* = 2^{-\frac{1}{8}} \varepsilon^{-\frac{3}{8}} S_{min}^{-\frac{1}{4}} k_{max}^{-\frac{3}{8}} \end{cases}$$

*asymptotically solve the min-max problem (5), and lead to the following estimate*

$$\max_{k \in \mathbb{K}} \hat{\rho}_{2C}(k, 0, q_1^*, q_2^*) = 1 - 2 \cdot 2^{\frac{5}{8}} \varepsilon^{-\frac{1}{8}} S_{min}^{\frac{1}{4}} k_{max}^{-\frac{1}{8}} + O(k_{max}^{-\frac{1}{4}}).$$

*Remark 1* A comparison between the results of Theorems 1 and 2 shows that when  $\delta < \frac{8}{5}$ , the presence of overlap does not enhance the performance of the OSWR algorithm with two-sided characteristic transmission conditions.

### 4 Numerical experiments

The theoretical findings are illustrated by solving the error equation derived from the viscoelastic model (1) in  $\Omega = (-1, 1)$ , with parameters  $\varepsilon = 2$ ,  $\gamma = 1$ , and  $T = 1$ . The domain is decomposed into  $\Omega_1 = (-1, l)$  and  $\Omega_2 = (l, 1)$ , with overlap  $L = 2h$  (i.e.  $l = h$ ) unless stated otherwise. The OSWR algorithm (2) is implemented with the centered finite difference in space and the Crank-Nicolson method in time. The algorithm starts from random initial guesses  $g_i^0 (i = 1, 2)$  and stops if  $\max\{\|g_1^n - g_1^{n-1}\|_\infty, \|g_2^n - g_2^{n-1}\|_\infty\} < 10^{-3}$ .

The convergence behavior of the OSWR algorithm with two-sided characteristic conditions using  $h = \frac{1}{40}, \frac{1}{80}, \dots, \frac{1}{640}$ , as shown in the left panel of Fig. 2, confirms the theoretical prediction from Theorem 1: the convergence factor behaves like  $1 - O(h^{\frac{1}{8}})$  for  $\tau = h$  and  $1 - O(h^{\frac{1}{5}})$  for  $\tau = h^2$ , but only for very small mesh size  $h$ .

By varying  $(q_1, q_2)$  for  $\varepsilon = 2$  under  $\tau = h = \frac{1}{500}$  and recording the resulting iteration counts, we observe in the middle plot of Fig. 2 that the theoretical values (marked by a red star) align well with the numerical optimum. And we believe that on finer grids the theoretical prediction would perform even better.

We now assess the robustness of the two-sided characteristic transmission condition to the damping coefficient  $\varepsilon$ . The right panel of Fig. 2, obtained with  $\tau = h = \frac{1}{1000}$ , clearly demonstrates the improved robustness of the two-sided characteristic condition: it performs comparably to the wave condition and significantly better than the Robin condition for small  $\varepsilon$ , while outperforming both for larger  $\varepsilon$

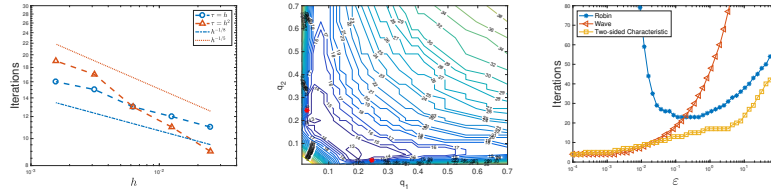


**Fig. 2** Left: the asymptotic behavior as the spatial grid is refined with the overlap  $L = 2h$ , together with the predicted convergence rates from analysis. Middle: optimized parameter (\*) found by asymptotic analysis, compared with the performance of other parameter values. Parameters:  $\varepsilon = 2$ ,  $\tau = h = \frac{1}{500}$ . Right: the number of iterations as a function of  $\varepsilon$  with  $L = 2h$ ,  $\tau = h = \frac{1}{1000}$ .

though the iteration count still increases in  $\varepsilon$  because of the nature of the problem itself. In contrast, the classical SWR method requires at least 259 iterations and grows significantly in  $\varepsilon$ . To sum up, the two-sided characteristic condition is more robust than the wave and Robin conditions, although its iteration count still increases in the damping coefficient  $\varepsilon$ . Furthermore, the iteration counts for varying  $\gamma$  are presented in Table 1 with  $h = \frac{1}{200}$ , showing that the algorithm is largely insensitive to  $\gamma$ .

**Table 1** The number of iterations for varying parameter  $\gamma$  with the overlap  $L = 2h$  and  $h = \frac{1}{200}$  for  $\tau = h$  and  $\tau = h^2$  (in brackets).

$\varepsilon \setminus \gamma$	$2^{-4}$	$2^{-2}$	$2^0$	$2^2$	$2^4$
0.02	9[7]	9[6]	7[5]	6[6]	6[9]
0.2	12[10]	11[9]	10[9]	9[7]	9[7]
2	14[15]	13[15]	13[15]	11[13]	15[13]

**Table 2** Iteration counts for the OSWR algorithm with two-sided characteristic transmission conditions for varying overlap  $L$  with  $h = \frac{1}{200}$ .

$L$	0	$2h$	$4h$	$8h$
$\tau = h$	13	13	13	12
$\tau = h^2$	26	15	11	9

Next, we investigate the influence of overlap size  $L$  on convergence using  $h = \frac{1}{200}$  and  $\tau = h$  or  $\tau = h^2$ . Using  $L = 0, 2h, 4h, 8h$ , Table 2 shows that for  $\tau = h^2$ , increasing overlap reduces iterations, whereas for  $\tau = h$ , overlap has negligible effect—consistent with Remark 1.

Finally, a many-subdomain case is tested, as shown in Table 3. The results indicate that more iterations are required when increasing the number of subdomains, especially for strong damping scenarios. Using the OSWR algorithm as a preconditioner [6] and introducing a coarse grid correction would enhance the scalability.

**Table 3** The number of iterations required by the OSWR algorithm with two-sided characteristic condition in many-subdomain case, with overlap  $L = 2h$ ,  $\tau = h$  and  $h = \frac{1}{128}$ . ‘#’ denotes the number of subdomains.

$\varepsilon \setminus \#$	2	4	8	16
0.02	6	8	11	16
0.2	9	10	19	47
2	13	33	101	180

## 5 Conclusion

Through an analysis of the convergence factor derived from Fourier analysis, a two-sided characteristic transmission condition is thus designed for the OSWR algorithm applied to the Kelvin–Voigt viscoelastic wave equation, with the objective of achieving robustness against damping. The resulting optimized algorithm demonstrates significantly improved robustness over all damping parameters within the investigated range, outperforming existing SWR methods. However, numerical observations indicate that the algorithm fails to achieve its optimal performance with relatively large mesh sizes (see the left plot of Fig. 2), a finding that merits further study. Furthermore, the case of variable damping and the design of a coarse grid correction, which are of great practical importance in many applications, also deserve future investigation.

**Acknowledgements** Partly supported by the Scientific Research Project of Education Department of Jilin Provincial JJKH20250297BS.

## References

1. Aki, K., Richards, P.G.: Quantitative seismology. University Science Books (2002)
2. Bennequin, D., Gander, M.J., Halpern, L.: A homographic best approximation problem with application to optimized Schwarz waveform relaxation. *Math. Comp.* **78**(265), 185–223 (2009)
3. Chouly, F., Gander, M.J., Martin, V.: Optimized Schwarz waveform relaxation methods for wave-heat coupling in one dimensional bounded domains. *Numer. Algorithms* **100**, 1739–1763 (2025)
4. Clement, S., Lemarié, F., Blayo, E.: Discrete analysis of Schwarz waveform relaxation for a diffusion reaction problem with discontinuous coefficients. *SMAI J. Comput. Math.* **8**, 99–124 (2022)
5. Ferry, J.D.: Viscoelastic properties of polymers. Wiley, United Kingdom (1980)
6. Gander, M.J., Gouarin, L., Halpern, L.: Optimized Schwarz waveform relaxation methods: A large scale numerical study. In: *Domain Decomposition Methods in Science and Engineering XIX*, pp. 261–268. Springer Berlin Heidelberg (2011)
7. Gander, M.J., Halpern, L.: Absorbing boundary conditions for the wave equation and parallel computing. *Math. Comp.* **74**(249), 153–176 (2005)
8. Gander, M.J., Halpern, L., Nataf, F.: Optimal Schwarz waveform relaxation for the one dimensional wave equation. *SIAM J. Numer. Anal.* **41**(5), 1643–1681 (2003)
9. Gander, M.J., Lunowa, S.B., Rohde, C.: Non-overlapping Schwarz waveform-relaxation for nonlinear advection-diffusion equations. *SIAM J. Sci. Comput.* **45**(1), A49–A73 (2023)
10. Gander, M.J., Stuart, A.M.: Space-time continuous analysis of waveform relaxation for the heat equation. *SIAM J. Sci. Comput.* **19**(6), 2014–2031 (1998)
11. Gander, M.J., Zhao, H.: Overlapping Schwarz waveform relaxation for parabolic problems in higher dimension. In: *Proceedings of Algorithm 14*, pp. 42–51. Slovak Tech. Univ. (1997)
12. Giladi, E., Keller, H.: Space-time domain decomposition for parabolic problems. *Appl. Math.* **217**, 50 (1997)
13. Hoang, T.T.P., Lee, H.: A global-in-time domain decomposition method for the coupled nonlinear Stokes and Darcy flows. *J. Sci. Comput.* **87**(1), 1–22 (2021)
14. Li, F., Xu, Y.: Which transmission condition is the best in optimized Schwarz waveform relaxation for viscoelastic equation: Robin or characteristic? Zenodo (2025)